

Organized Grouped Discrete Representation for Object-Centric Learning

Rongzhen Zhao, Vivienne Wang, Juho Kannala, Joni Pajarinen

{rongzhen.zhao, vivienne.wang, juho.kannala, joni.pajarinen}@aalto.fi

Aalto University, Espoo 02150, Finland

Abstract

Object-Centric Learning (OCL) represents dense image or video pixels as sparse object features. Representative methods utilize discrete representation composed of Variational Autoencoder (VAE) template features to suppress pixel-level information redundancy and guide object-level feature aggregation. The most recent advancement, Grouped Discrete Representation (GDR), further decomposes these template features into attributes. However, its naive channel grouping as decomposition may erroneously group channels belonging to different attributes together and discretize them as sub-optimal template attributes, which losses information and harms expressivity. We propose *Organized* GDR (OGDR) to organize channels belonging to the same attributes together for correct decomposition from features into attributes. In unsupervised segmentation experiments, OGDR is fully superior to GDR in augmentating classical transformer-based OCL methods; it even improves state-of-the-art diffusion-based ones. Codebook PCA and representation similarity analyses show that compared with GDR, our OGDR eliminates redundancy and preserves information better for guiding object representation learning. The source code is available in the supplementary material.

Introduction

Under self or weak supervision, Object Centric Learning (OCL) (Greff et al. 2019; Burgess et al. 2019) can represent dense image or video pixels as sparse object feature vectors, with corresponding segmentation masks as byproducts that reflect how well the object features are. This is metaphysically bio-plausible, because we humans perceive visual scenes as objects for higher-level vision cognition, like understanding, reasoning, planning, and decision-making (Bar 2004; Cavanagh 2011; Palmeri and Gauthier 2004). This is also physically desired, because object-level representation of images or videos is more versatile for visual tasks involving different modalities (Yi et al. 2020; Wu et al. 2023a).

Representative OCL includes the ones that are mixture-based (Locatello et al. 2020; Kipf et al. 2022), transformer-based (Singh, Deng, and Ahn 2022; Singh, Wu, and Ahn 2022), foundation-based (Seitzer et al. 2023; Zadaianchuk, Seitzer, and Martius 2024) and diffusion-based (Wu et al. 2023b; Jiang et al. 2023). The latter three all utilize intermediate representation to suppress inter-pixel dissimilarities

and enhance intra-object similarities so as to guide object-level feature aggregation. For the transformer and diffusion-based ones, such guidance is obtained by representing images or videos with template features from a pretrained Variational Autoencoder (VAE) (Singh, Deng, and Ahn 2022; Van Den Oord, Vinyals, and Kavukcuoglu 2017) codebook. Such codes are in limited number and shared across the dataset. The most recent work GDR (Zhao et al. 2024) further decomposes those template features into more reusable attributes. This suppresses inter-pixel dissimilarity and enhances intra-object similarity more, achieving better performance and generalization on transformer-based baselines.

However, GDR’s *naive channel grouping* on intermediate representation *as the decomposition* from features to attributes, neglects the fact that channels belonging to the same attribute may scatter among all channel places rather than together in one adjacent channel group. In other words, **as shown in Fig. 1**, channels belonging to different attributes are grouped together and discretized into sub-optimal template attributes, which loses information and damages model expressivity. Besides, GDR only works on transformer-based methods, not diffusion-based ones.

We propose (i) *Organized* Grouped Discrete Representation (OGDR), which organizes intermediate representation channels for grouped discretization, overcoming the information loss and model expressivity damage. (ii) OGDR is applicable not only to classical transformer-based methods, but also to state-of-the-art diffusion-based ones. (iii) Comprehensive experiments demonstrate how well OGDR improves the baselines. (iv) Intuitive analyses illustrate statistically and visually how OGDR channel organizing augments model expressivity and guides object representation learning. (v) Ablation studies show how to configure the hyperparameters and maximize OGDR’s effectiveness.

Related Work

Object Centric Learning (OCL). Mainstream OCL utilizes SlotAttention (Locatello et al. 2020; Bahdanau, Cho, and Bengio 2015) to aggregate dense feature maps into sparse object features, and further utilizes intermediate representation, which suppresses pixel-level redundant details, to handle textured objects. Transformer-based OCL, like SLATE (Singh, Deng, and Ahn 2022) and STEVE (Singh, Wu, and Ahn 2022), generates input tokens from slots via a trans-

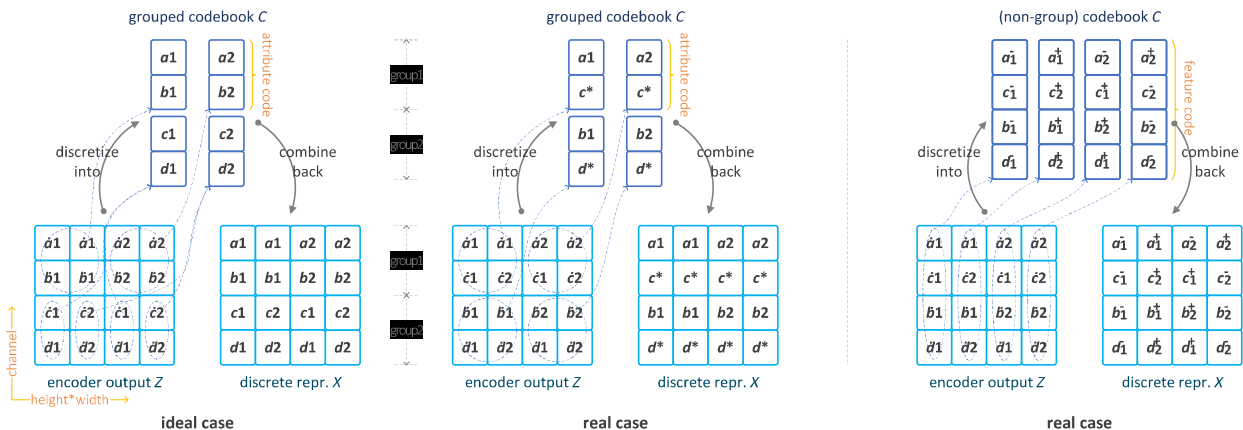


Figure 1: Problem. Naive grouped discretization loses information (*left*) while non-grouped discretization retains redundancy (*right*). Suppose a dataset can be fully represented by four template features, which can be decomposed into two attribute groups, each with two fundamental template attributes: $(a_1, b_1)^T$ and $(a_2, b_2)^T$, $(c_1, d_1)^T$ and $(c_2, d_2)^T$; Channels a and b form one attribute, c and d another; Arbitrary continuous values $\hat{a}_1, \hat{a}_2, \dots, \hat{d}_2$ should be ideally discretized into a_1, a_2, \dots, d_2 , respectively. In the **grouped ideal case**, for Z of channel order a - b - c - d , direct two-grouping puts channels belong to the same attribute together. Thus continuous attribute $(\hat{a}_1, \hat{b}_1)^T$ can be discretized into template attribute $(a_1, b_1)^T$, and so do the others. The resulting grouped discrete representation X ideally represents Z . In a **grouped real case**, for Z of channel order a - c - b - d , naive grouping puts channels a and c together, which belong to different attributes. Thus continuous attributes $(\hat{a}_1, \hat{c}_1)^T$ and $(\hat{a}_1, \hat{c}_2)^T$ are discretized into (a_1, c_*) , where c_* is the mean of c_1 and c_2 . The resulting X loses some information of Z and damages model expressivity. In all **non-grouped real cases**, regardless of the channel order, every continuous feature in Z , e.g., $(\hat{a}_1, \hat{c}_1, \hat{b}_1, \hat{d}_1)$ is discretized into a template feature in C , e.g., $(\hat{a}_1, \hat{c}_1, \hat{b}_1, \hat{d}_1)^T$, where \hat{a}_1^- is some smaller value of a_1 . The resulting non-grouped discrete representation X does not lose information of Z but leaves over too much redundancy.

former decoder (Vaswani et al. 2017), guided by dVAE (Singh, Deng, and Ahn 2022) discrete representation (Fig. 2 first row left); Diffusion-based OCL, like SlotDiffusion (Wu et al. 2023b) and LSD (Jiang et al. 2023), recovers input noise from slots via a diffusion model (Rombach et al. 2022), guided by VQ-VAE (Van Den Oord, Vinyals, and Kavukcuoglu 2017) discrete representation (Fig. 2 first row right); Foundation-based OCL, like DINOSAUR (Seitzer et al. 2023) and VideoSAUR (Zadaianchuk, Seitzer, and Martius 2024), reconstructs input features from slots via a spatial broadcast decoder (Watters et al. 2019), guided by well-pretrained features of the foundation model DINO (Caron et al. 2021; Oquab et al. 2023). We focus on VAE part of transformer- and diffusion-based methods.

Variational Autoencoder (VAE). dVAE (Singh, Deng, and Ahn 2022) is adopted in classical transformer-based OCL (Singh, Deng, and Ahn 2022; Singh, Wu, and Ahn 2022), to discretize intermediate representation of its encoder output by selecting template features in a codebook with hard Gumbel sampling (Jang, Gu, and Poole 2017) (Fig. 2 second row left). VQ-VAE (Van Den Oord, Vinyals, and Kavukcuoglu 2017) is employed in state-of-the-art diffusion-based OCL (Jiang et al. 2023; Wu et al. 2023b), to discretize intermediate representation by replacing features with the most similar codebook codes (Fig. 2 second row right). Techniques of other VAE variants, like grouping (Yang et al. 2023), residual (Barnes, Rizvi, and Nasrabadi 1996) and clustering (Lim, Jiang, and Yi 2020), are also worth exploiting for better discrete intermediate rep-

resentation to guide object-centric representation learning. We borrow some ideas from them.

Channel Grouping. Splitting features along the channel dimension and transforming them separately is often used to promote representation diversity (Krizhevsky, Sutskever, and Hinton 2012; Chen et al. 2019; Huang et al. 2018; Zhao, Wu, and Zhang 2021; Zhao, Li, and Wu 2022). This is also explored in OCL. SysBinder (Singh, Kim, and Ahn 2022) groups slot queries into different “blocks” to aggregate different attributes of objects, yielding more interpretability in object representation but limited performance boosts. The most recent OCL augmentor GDR (Zhao et al. 2024) groups the VAE discrete representation into combinatorial template attributes, to guide object feature aggregation in transformer-based methods (Fig. 2 second row center). It augments baselines in both performance and generalization, but its naive channel grouping as decomposition somehow harms model expressivity. Our OGDR is more beneficial to both transformer- and diffusion-based methods.

Proposed Method

We propose *Organized* Grouped Discrete Representation (OGDR), a general augmentor to representative OCL methods like the transformer-based (Singh, Deng, and Ahn 2022; Singh, Wu, and Ahn 2022) and the diffusion-based (Wu et al. 2023b; Jiang et al. 2023).

Notations: image or video frame I , continuous representation Z , discrete representation X , and noise N are ten-

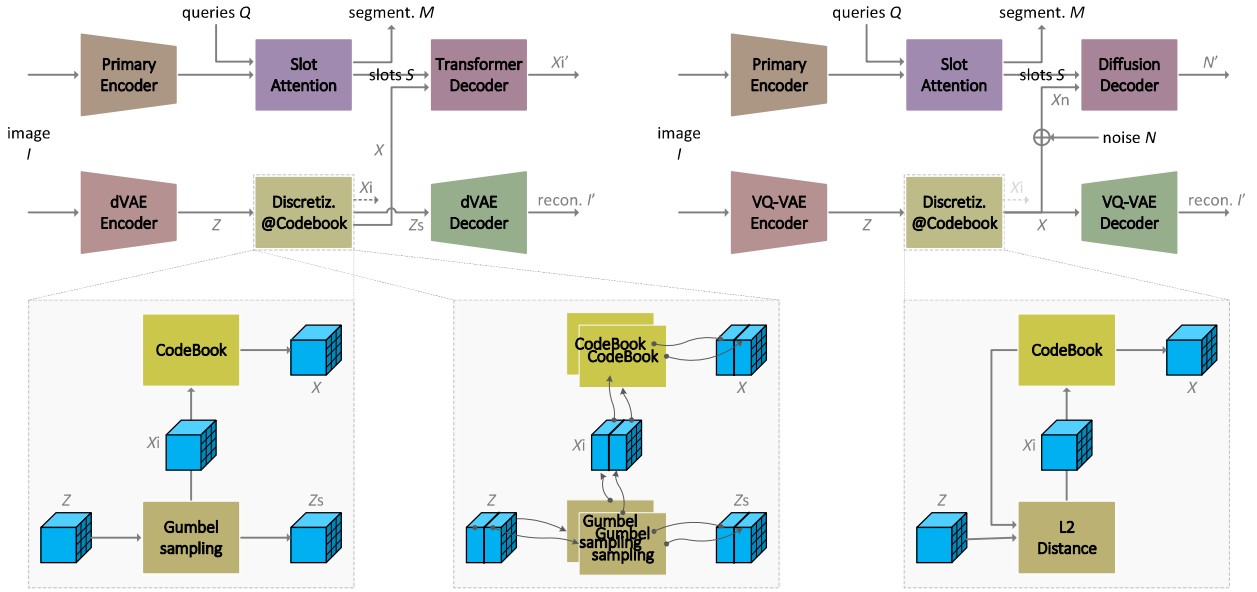


Figure 2: Preliminary. First row: model architectures of transformer-based OCL (left) and diffusion-based OCL (right). Second row: non-grouped intermediate representation discretization in dVAE (left), grouped discrete representation in dVAE (GDR) (center), and non-grouped discretization in VQ-VAE (right). GDR can be extended to VQ-VAE.

sors in shape (height, width, channel); queries Q and slots S are tensors in shape (number, channel); segmentation M is a tensor in shape (height, width).

Preliminary: Discrete Representation

Both transformer-based classics and diffusion-based state-of-the-arts learn to extract object features (slots) from images or videos, guided by their discrete representation.

Transformer-based architecture is drawn in Fig. 2 first row left. Input image or video frame I is encoded by a primary encoder and aggregated by SlotAttention (Locatello et al. 2020) into slots S under queries Q , with objects (and the background) segmentation masks M as byproducts. Meanwhile, a pretrained VAE model represents I as discrete X and the corresponding code indexes X_i . Afterwards, with a transformer decoder, S is challenged to reconstruct X_i as classification guided by causally masked X . For video modality, current slots S is transformed by a transformer encoder block into queries for next frame.

Specifically, discrete representation for transformer-based OCL is obtained as in Fig. 2 second row left:

(i) predefine a codebook C holding n c -dimensional learnable codes as template features; (ii) transform input I with dVAE encoder into continuous intermediate representation Z ; (iii) sample Z via Gumbel and yield one-hot indexes X_i , with soft sampling Z_s for dVAE decoding; (iv) index template features from C by X_i and compose the discrete representation X .

Diffusion-based architecture is drawn in Fig. 2 first row right. The only difference is that with a conditional diffusion model decoder, S is challenged to reconstruct Gaussian noise N being added as regression, guided by X .

Specifically, discrete representation for diffusion-based OCL is obtained as in Fig. 2 second row right:

(i) predefine a codebook C holding n learnable codes as template features; (ii) transform input I with VQ-VAE encoder into continuous intermediate representation Z ; (iii) find the most similar code indexes X_i in C for every superpixel in Z by least L2 distance; (iv) select template features in C by X_i to form discrete representation X , which is also for VQ-VAE decoding.

The **guidance** here means that with X as cues and S as conditions, a transformer or diffusion decoder strives to reconstruct I , which forces S to extract as much object information as possible. The key is suppressing texture noises with X and enhancing object feature consistency.

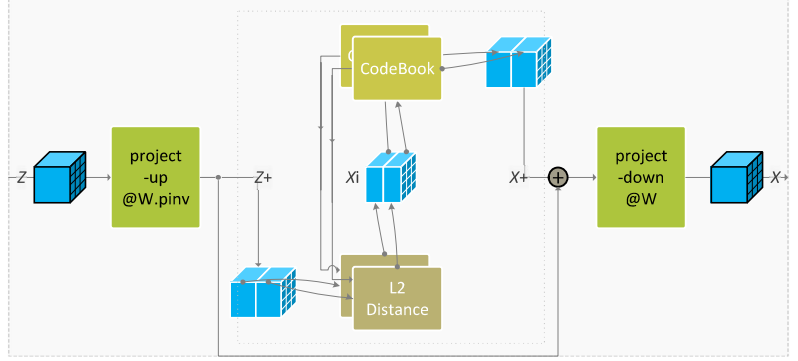
Naive Grouped Discrete Representation

GDR or Grouped Discrete Representation (Zhao et al. 2024) is based on dVAE and only works for transformer-based OCL. Its naive channel grouping as decomposition from features to attributes enhances the aforementioned guidance but harms model expressivity.

Similar to Fig. 2 second row center, we unify the VAE part of both transformer-based and diffusion-based methods with VQ-VAE, and transfer such naive GDR technique to VQ-VAE. This yields a general OCL augmentor because after pretraining, VQ-VAE provides the already learnt discrete representation required by the diffusion.

Beforehand, suppose a dataset is fully described by n c -dimensional template features that are fully described by g attribute groups, each of which has a d -dimensional template attributes. Here $n == a^g$ and $c == g \times d$. Accordingly, we predefine a set of attribute codebooks $C =$

Figure 3: Solution. Organized grouped discrete representation (OGDR) is obtained by (i) projecting Z up in channel dimension with pseudo-inverse of matrix W ; (ii) conducting naive channel grouping and discretization by L2 distance upon attribute codes from Z_+ into X_+ and code indexes X_i ; (iii) adding residual Z_+ to X_+ for pretraining only; (iv) projecting X_+ down in channel dimension with learnable matrix W into X ; and (v) normalizing X finally.



$\{C^{(1)}, C^{(2)} \dots C^{(g)}\}$, whose codes parameters are in shape (g, a, d) . Ideally, the combinations of those attribute-level codebooks are equivalent to the non-grouped feature-level codebook, whose code parameters are in shape (n, d) .

This is the same for both dVAE and VQ-VAE.

Afterwards, we transform input I with VAE encoder into continuous intermediate representation Z .

For grouped discretization, in dVAE, GDR samples Z via Gumbel noise (Jang, Gu, and Poole 2017) and yields tuple code indexes X_i , along with soft sampling Z_s :

$$Z_s = \text{softmax}\left(\frac{Z^{(1)} + G}{\tau}\right) \parallel \text{softmax}\left(\frac{Z^{(2)} + G}{\tau}\right) \parallel \dots \parallel \text{softmax}\left(\frac{Z^{(g)} + G}{\tau}\right) \quad (1)$$

$$X_i = \text{argmax}(Z_s^{(1)}) \parallel \text{argmax}(Z_s^{(2)}) \parallel \dots \parallel \text{argmax}(Z_s^{(g)}) \quad (2)$$

where $Z^{(1)} \dots Z^{(g)}$ are channel groups of Z ; noise $G \sim \text{Gumbel}(\mu = 0, \beta = 1)$, with temperature τ ; \parallel is channel concatenation; $\text{argmax}(\cdot)$ is along the channel dimension.

But in VQ-VAE, we sample distances between Z and C via Gumbel noise and yield tuple code indexes X_i :

$$D = \text{l2}(Z^{(1)}, C^{(1)}) \parallel \text{l2}(Z^{(2)}, C^{(2)}) \parallel \dots \parallel \text{l2}(Z^{(g)}, C^{(g)}) \quad (3)$$

$$D_s = \text{softmax}\left(\frac{D^{(1)} + G}{\tau}\right) \parallel \text{softmax}\left(\frac{D^{(2)} + G}{\tau}\right) \parallel \dots \parallel \text{softmax}\left(\frac{D^{(g)} + G}{\tau}\right) \quad (4)$$

$$X_i = \text{argmin}(D_s^{(1)}) \parallel \text{argmin}(D_s^{(2)}) \parallel \dots \parallel \text{argmin}(D_s^{(g)}) \quad (5)$$

where $\text{l2}(\cdot, \cdot)$ means L2 distances between every vector pair in its two arguments; D_s is soft Gumbel sampling of distances D between continuous representations and codes; $\text{argmin}(\cdot)$ is along the code dimension.

Subsequently, index template attributes by X_i from C and form grouped discrete representation X ; transform X_i from tuple into scalar format:

$$X = \text{index}(C^{(1)}, X_i^{(1)}) \parallel \text{index}(C^{(2)}, X_i^{(2)}) \parallel \dots \parallel \text{index}(C^{(g)}, X_i^{(g)}) \quad (6)$$

$$X_i := a^0 \times X_i^{(1)} + a^1 \times X_i^{(2)} + \dots + a^{(g-1)} \times X_i^{(g)} \quad (7)$$

where $X_i^{(1)} \dots X_i^{(g)}$ are channel groups of X_i ; and $\text{index}(\cdot, \cdot)$ selects codes from a codebook by indexes.

This is the same for both dVAE and VQ-VAE.

Finally, as for pretraining supervision, we also add the utilization loss proposed in GDR to the VQ-VAE setting. The number of *groups* and corresponding codebook *parameters* are similar to those of GDR.

However, information loss and model expressivity damage caused by the naive channel grouping as decomposition, as shown in Fig. 1, remain unaddressed.

Organized Grouped Discrete Representation

As shown in Fig. 3, we propose organized grouping to replace the naive channel grouping of GDR. The *key idea* is: use a invertible projection to organize channels of the continuous intermediate representation for better grouped discretization with less information loss; then use this projection to recover the (discrete) intermediate representation. In return, less information loss leads to better model expressivity, and ultimately better OCL guidance.

Firstly, we project the intermediate representation Z up to higher channel dimension with the pseudo-inverse of a learnable matrix W :

$$Z_+ = Z \cdot \text{pinv}(W) \quad (8)$$

where Z is in shape (height, width, channel= c); $\text{pinv}(\cdot)$ is the pseudo-inverse operation; and matrix $\text{pinv}(W)$ is in shape (channel= c , expanded channel= $8c$).

This facilitates channels belonging to the same attributes to be placed together (i) by allowing channel reordering through such transformation and (ii) by producing more channel replicas to counteract mis-grouping.

Secondly, group the expanded representation Z_+ along the channel dimension and discretize it by L2 distance upon the attribute-level codebooks C . Accordingly, we get code indexes X_i and the expanded discrete representation X_+ . This is already formulated above in Eq. 3-7, with only different notations of Z vs Z_+ and X vs X_+ .

Meanwhile, add Z_+ to X_+ :

$$X_+ := Z_+ \times \alpha + X_+ \times (1 - \alpha) \quad (9)$$

where α is decayed by cosine annealing¹ from 0.5 to 0 in the former half pretraining, and is fixed to 0 after training.

¹https://pytorch.org/docs/stable/generated/torch.optim.lr_scheduler.CosineAnnealingLR.html

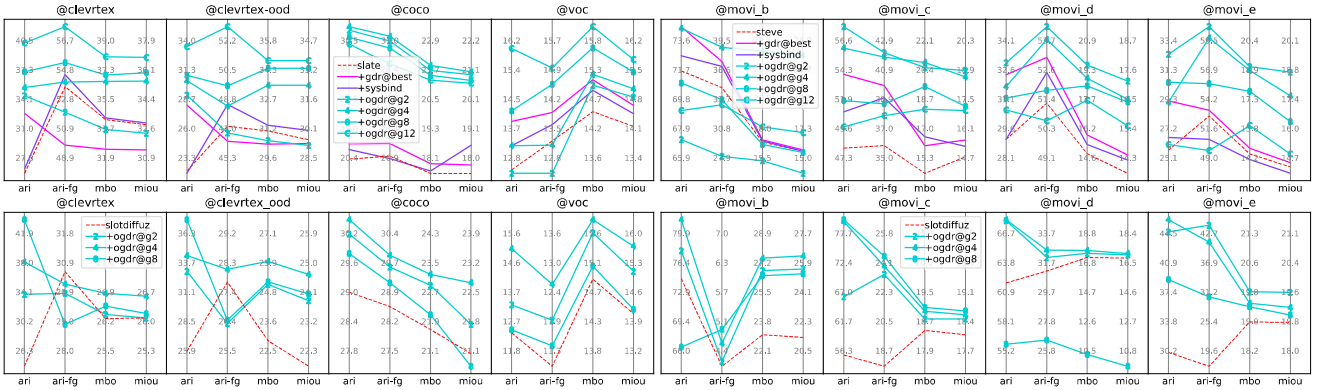


Figure 4: **OGDR** boosts both transformer-based (*top*) and diffusion-based (*bottom*) methods in OCL performance measured by unsupervised segmentation on images (*left*) or videos (*right*). The primary encoder is unified as a four-layer naive CNN. Titles are datasets; x ticks are metrics while y ticks are metric values in adaptive scope; $g2/4/8/12$ are OGDR groups numbers.

With such residual preserving information from continuous to discrete, the whole VAE can be pretrained sufficiently even if bad grouped discretization loses information.

Thirdly, project the expanded discrete representation X_+ down and yield the final organized grouped discrete representation X , as a recovery of Z :

$$X = X_+ \cdot W \quad (10)$$

where W is the aforementioned learnable matrix in shape (expanded channel= $8c$, channel= c).

Such parameter-sharing project-up and project-down enforce strong inductive bias on the organizing. Specified parameters as project-up worsens the performance.

Finally, in case of numerical instability due to matrix multiplication of pseudo-inverse, we normalize X :

$$X := \frac{X - \mathbb{E}[X]}{\sqrt{\mathbb{V}[X] + \epsilon}} \quad (11)$$

where \mathbb{E} and \mathbb{V} are mean and variance over height, width and channel; ϵ is a small number to avoid zero-division.

Hyper-parameter setting. We use typical codebook size $n=4096$, and typical channel dimension $c=256$ for transformer-based methods while $c=4$ for diffusion-based methods. Similar to GDR, group numbers can be $g2, 4, 8$ and 12 ; channel expansion rate is by default set to $8c$. Same as GDR, the corresponding available parameters are still much less than the non-grouped codebook, as grouping itself saves many times of parameters in codebook, which leaves budget for our project-up and project-down design.

Experiments

We evaluate these points with our experiments: (i) OGDR beats GDR and augments both transformer-based and diffusion-based OCL; (ii) OGDR improves OCL model expressivity while enhancing OCL guidance; (iii) Components of OGDR contribute to its success and how to set them.

OCL Performance

We cover the following recognized cases to evaluate object-centric learning performance with 3 random seeds.

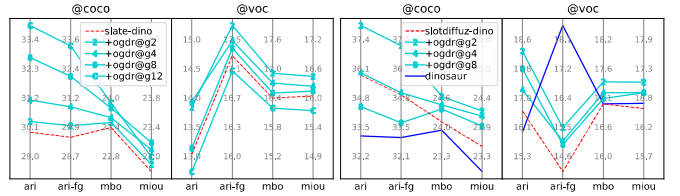


Figure 5: **OGDR** still improves both transformer-based (left) and diffusion-based (right) methods even with the foundational model DINO as the strong primary encoder.

The transformer-based models are SLATE (Singh, Deng, and Ahn 2022) for image and STEVE (Singh, Wu, and Ahn 2022) for video; the diffusion-based models are SlotDiffusion (Wu et al. 2023b) for image and its temporal variant for video. Our competitors, SysBinder (Singh, Kim, and Ahn 2022) @ $g4$ and GDR (Zhao et al. 2024) @best, are reported. DINOSAUR (Seitzer et al. 2023), the foundation-based, is also included as a reference. Naive CNN (Kipf et al. 2022; Elsayed et al. 2022) is used as a unified primary encoder.

The datasets are ClevrTex², COCO³ and VOC⁴ for image OCL, and MOVi-B/C/D/E⁵ for video OCL. They cover both synthetic and real-world cases, and each scene contains multiple objects with textures of different difficulty levels. Data processing follows the conventions.

The metrics are Adjusted Rand Index (ARI)⁶, ARI_{fg} (ARI foreground), mean Best Overlap (mBO)⁷ and mean Intersection-over-Union (mIoU)⁸ of the accuracy of the

²<https://www.robots.ox.ac.uk/~vggg/data/clevertex>

³<https://cocodataset.org/#panoptic-2020>

⁴<http://host.robots.ox.ac.uk/pascal/VOC>

⁵https://github.com/google-research/kubric/tree/main/challenge_s/movi

⁶https://scikit-learn.org/stable/modules/generated/sklearn.metrics.adjusted_rand_score.html

⁷<https://ieeexplore.ieee.org/document/7423791>

⁸https://scikit-learn.org/stable/modules/generated/sklearn.metrics.jaccard_score.html

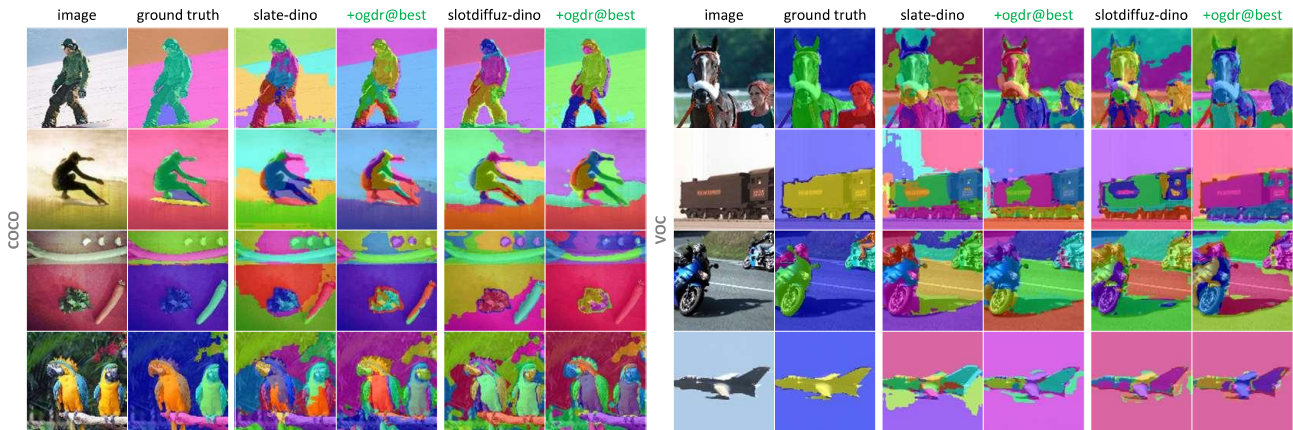


Figure 6: Qualitative results of SLATE-DINO and SlotDiffusion-DINO plus OGDR on COCO (left) and VOC (right).

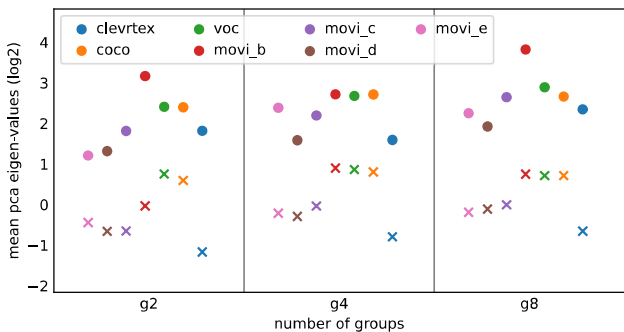


Figure 7: VAE codebook diversity measured by PCA eigen-values mean (y axis) of template features in codebook. Circles are results of our OGDR and crosses are GDR; different colors mean different datasets; the higher the better.

byproduct unsupervised segmentation, as the measurement of object-centric representation learning quality.

Results are shown in Fig. 4. In most cases of synthetic or real-world images or videos, our OGDR boosts OCL performance of both transformer-based classics (SLATE and STEVE) and diffusion-based state-of-the-arts (SlotDiffusion) significantly, while GDR is only applicable to the transformer-based. Upon SLATE and STEVE, OGDR beats the competitive augmentors, SysBinder and GDR, by a large margin on all datasets except MOVi-B.

We also evaluate OGDR upon these models with foundation model DINO (Caron et al. 2021) as strong primary encoder, along with DINOSAUR, as shown in Fig. 5 and 6. On either SLATE or SlotDiffusion, OGDR still boosts their OCL performance under all metrics in most cases. Particularly, OGDR even makes the old SLATE as competitive as the advanced SlotDiffusion on COCO.

Model Expressivity

We argue that our OGDR preserves information when suppressing redundancy, namely, yielding better model expressivity than GDR. This can be measured (i) by template fea-

tures diversity in VAE codebook and (ii) by object discriminability in VAE discrete representation.

As shown in Fig. 7, OGDR codebook diversity is significantly higher than that of GDR, by counting the mean of PCA (Principal Component Analysis)⁹ eigen-values of VAE codebook. Our organizing technique promotes the VAE model to grasp more diverse template features for better representation discretization. As shown in Fig. 8, OGDR object discriminability is obviously clearer than that of GDR, by coloring superpixels according to their cosine similarities¹⁰. Our organizing technique fosters better guiding representation for object representation learning.

More **interpretable** visualizations about channel organizing and discrete representation are provided in the appendix.

Ablation

The effects of designs in OGDR are listed in Fig. 1. We use the VAE pretraining performance, measured in reconstruction MSE, as the metrics for easy comparison.

Number of groups formulated in Eq. 3⁷: $g=2, 4, 8$ or 12 . As already drawn in Eq. 4 and 5, the best g is dependent on specific datasets, yet $g12$ is more likely to have lower performance than the baselines.

Channel expansion rate of the project-up formulated in Eq. 8: $c, 2c, 4c$ or $8c$. For transformer-based methods, although $8c$ usually works the best, the expansion rate for OGDR has little impact on the performance. This implies that our organizing truly works, making higher channel expansion rate contribute less to grouping channels belonging to the same attribute together. By contrast, high expansion rate is important for the diffusion-based, because the intermediate channel dimension is only 4, much less than that of the transformer-based, which is 256.

Pseudo-inverse of W as the *project-up* vs specified weights formulated in Eq. 8. We use specified weights as

⁹<https://scikit-learn.org/stable/modules/generated/sklearn.decomposition.PCA.html>

¹⁰https://scikit-learn.org/stable/modules/generated/sklearn.metrics.pairwise.cosine_similarity.html

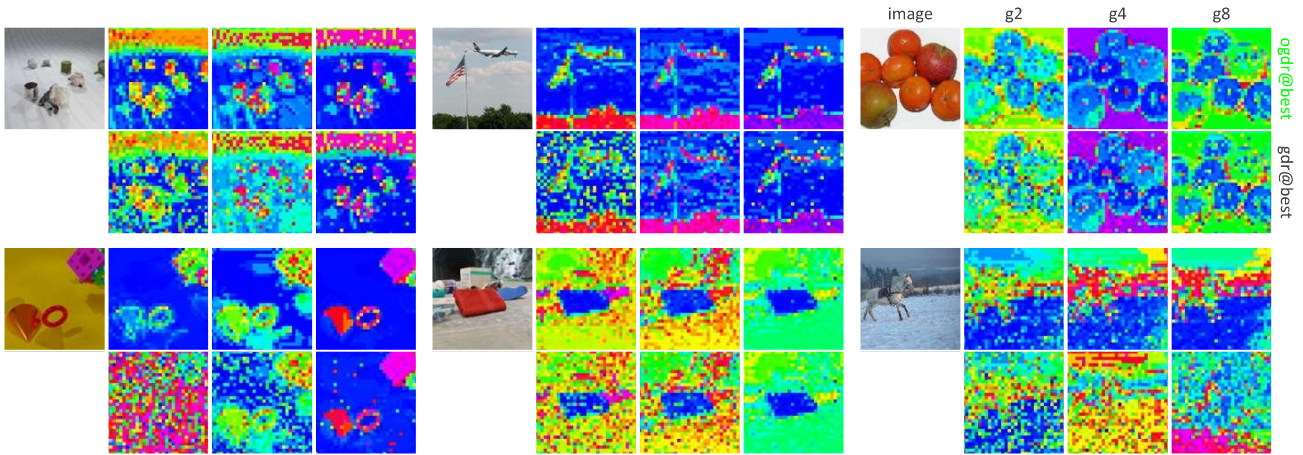


Figure 8: Object discriminability in VAE discrete representation by cosine similarity between superpixels and the central superpixel. Similar colors mean bigger similarity. Under group numbers 2/4/8, OGDG eliminates more pixel redundancy and preserves more object consistency thus provides clearer guidance to object representation learning than GDR does.

vqvae+ogdr@g4	expansion rate			
	8c	4c	2c	1c
c256-clevrtex	0.0078	0.0075	0.0083	0.0079
c256-coco	0.0187	0.0191	0.0194	0.0192
c4-clevrtex	0.0102	0.0114	0.0132	0.0151
c4-coco	0.0233	0.0241	0.0261	0.0298
vqvae+ogdr@g4	best setting	project-up pinv.→spec.	residual w.→w.o.	normaliz w.→w.o.
c256-clevrtex	0.0078	0.0081	0.0081	0.0079
c256-coco	0.0187	0.0188	0.0189	0.0188
c4-clevrtex	0.0102	0.0103	0.0132	0.0132
c4-coco	0.0233	0.0237	0.0317	0.0251

Table 1: Ablation studies measured by pretraining VAE reconstruction MSE. “c256” means VAE with intermediate channel dimension 256 for transformer-based methods and “c4” is 4 intermediate channels for diffusion-based ones; “g4” is that we use grouping number 4 as examples. “pinv.→spec.” means the project-up with specified weights, rather than pseudo-inverse of the project-down. “w.→w.o.” means removing the residual or normalization technique.

the project-up rather than using the pseudo-inverse of the project-down, but this mostly does harm to the performance. This again proves our design really organizes the channels for attribute decomposed grouping.

Using annealing *residual connection* formulated in Eq. 9 is always beneficial than not.

Normalization at last formulated in Eq. 11 is usually beneficial for diffusion-based OCL methods, but it has no obvious effect on transformer-based methods.

Conclusion

We propose organized grouped discrete representation technique to guide Object-Centric Learning better. Our tech-

nique outperforms the naive grouped discrete representation technique, and is applicable to both transformer-based OCL methods and diffusion-based ones. By statistical and visual analysis, we show that our organizing design truly facilitates channel grouping as decomposition from features to attributes, thus improving model expressivity and object representation learning guidance. Similar to GDR, there are some issues in our technique, like lower code utilization along with more groups and more hyper-parameters to tune in pretraining. These may be solved by borrowing ideas from VAE-related researches, which are left for future work.

References

- Bahdanau, D.; Cho, K. H.; and Bengio, Y. 2015. Neural Machine Translation by Jointly Learning to Align and Translate. *International Conference on Learning Representations*.
- Bar, M. 2004. Visual Objects in Context. *Nature Reviews Neuroscience*, 5(8): 617–629.
- Barnes, C.; Rizvi, S.; and Nasrabadi, N. 1996. Advances in Residual Vector Quantization: A Review. *IEEE Transactions on Image Processing*, 5(2): 226–262.
- Burgess, C.; Matthey, L.; Watters, N.; et al. 2019. MONet: Unsupervised Scene Decomposition and Representation. *arXiv preprint arXiv:1901.11390*.
- Caron, M.; Touvron, H.; Misra, I.; et al. 2021. Emerging Properties in Self-Supervised Vision Transformers. In *Proceedings of the IEEE/CVF International Conference on Computer Vision*, 9650–9660.
- Cavanagh, P. 2011. Visual Cognition. *Vision Research*, 51(13): 1538–1551.
- Chen, Y.; Fan, H.; Xu, B.; et al. 2019. Drop an Octave: Reducing Spatial Redundancy in Convolutional Neural Networks With Octave Convolution. In *Proceedings of the IEEE/CVF International Conference on Computer Vision*, 3435–3444.

- Elsayed, G.; Mahendran, A.; Van Steenkiste, S.; et al. 2022. SAVi++: Towards End-to-End Object-Centric Learning from Real-World Videos. *Advances in Neural Information Processing Systems*, 35: 28940–28954.
- Greff, K.; Kaufman, R. L.; Kabra, R.; et al. 2019. Multi-Object Representation Learning with Iterative Variational Inference. In *International Conference on Machine Learning*, 2424–2433. PMLR.
- Huang, G.; Liu, S.; Van der Maaten, L.; and Weinberger, K. 2018. CondenseNet: An Efficient DenseNet Using Learned Group Convolutions. In *Proceedings of the IEEE Conference on Computer Vision and Pattern Recognition*, 2752–2761.
- Jang, E.; Gu, S.; and Poole, B. 2017. Categorical Reparameterization with Gumbel-Softmax. *International Conference on Learning Representations*.
- Jiang, J.; Deng, F.; Singh, G.; and Ahn, S. 2023. Object-Centric Slot Diffusion. *Advances in Neural Information Processing Systems*.
- Kipf, T.; Elsayed, G.; Mahendran, A.; et al. 2022. Conditional Object-Centric Learning from Video. *International Conference on Learning Representations*.
- Krizhevsky, A.; Sutskever, I.; and Hinton, G. 2012. ImageNet Classification with Deep Convolutional Neural Networks. *Advances in Neural Information Processing Systems*, 25.
- Lim, K.-L.; Jiang, X.; and Yi, C. 2020. Deep Clustering with Variational Autoencoder. *IEEE Signal Processing Letters*, 27: 231–235.
- Locatello, F.; Weissenborn, D.; Unterthiner, T.; et al. 2020. Object-Centric Learning with Slot Attention. *Advances in Neural Information Processing Systems*, 33: 11525–11538.
- Oquab, M.; Darcet, T.; Moutakanni, T.; et al. 2023. DINOv2: Learning Robust Visual Features without Supervision. *Transactions on Machine Learning Research*.
- Palmeri, T.; and Gauthier, I. 2004. Visual Object Understanding. *Nature Reviews Neuroscience*, 5(4): 291–303.
- Rombach, R.; Blattmann, A.; Lorenz, D.; Esser, P.; and Ommer, B. 2022. High-Resolution Image Synthesis with Latent Diffusion Models. In *Proceedings of the IEEE/CVF Conference on Computer Vision and Pattern Recognition*, 10684–10695.
- Seitzer, M.; Horn, M.; Zadaianchuk, A.; et al. 2023. Bridging the Gap to Real-World Object-Centric Learning. *International Conference on Learning Representations*.
- Singh, G.; Deng, F.; and Ahn, S. 2022. Illiterate DALL-E Learns to Compose. *International Conference on Learning Representations*.
- Singh, G.; Kim, Y.; and Ahn, S. 2022. Neural Systematic Binder. *International Conference on Learning Representations*.
- Singh, G.; Wu, Y.-F.; and Ahn, S. 2022. Simple Unsupervised Object-Centric Learning for Complex and Naturalistic Videos. *Advances in Neural Information Processing Systems*, 35: 18181–18196.
- Van Den Oord, A.; Vinyals, O.; and Kavukcuoglu, K. 2017. Neural Discrete Representation Learning. *Advances in Neural Information Processing Systems*, 30.
- Vaswani, A.; Shazeer, N.; Parmar, N.; et al. 2017. Attention Is All You Need. *Advances in Neural Information Processing Systems*, 30.
- Watters, N.; Matthey, L.; Burgess, C.; and Alexander, L. 2019. Spatial Broadcast Decoder: A Simple Architecture for Disentangled Representations in VAEs. *ICLR 2019 Workshop LLD*.
- Wu, Z.; Dvornik, N.; Greff, K.; Kipf, T.; and Garg, A. 2023a. SlotFormer: Unsupervised Visual Dynamics Simulation with Object-Centric Models. *International Conference on Learning Representations*.
- Wu, Z.; Hu, J.; Lu, W.; Gilitschenski, I.; and Garg, A. 2023b. SlotDiffusion: Object-Centric Generative Modeling with Diffusion Models. *Advances in Neural Information Processing Systems*, 36: 50932–50958.
- Yang, D.; Liu, S.; Huang, R.; et al. 2023. Hifi-Codec: Group-Residual Vector Quantization for High Fidelity Audio Codec. *arXiv preprint arXiv:2305.02765*.
- Yi, K.; Gan, C.; Li, Y.; Kohli, P.; et al. 2020. CLEVRER: CoLLision Events for Video REpresentation and Reasoning. *International Conference on Learning Representations*.
- Zadaianchuk, A.; Seitzer, M.; and Martius, G. 2024. Object-Centric Learning for Real-World Videos by Predicting Temporal Feature Similarities. *Advances in Neural Information Processing Systems*, 36.
- Zhao, R.; Li, J.; and Wu, Z. 2022. Convolution of Convolution: Let Kernels Spatially Collaborate. In *Proceedings of the IEEE/CVF Conference on Computer Vision and Pattern Recognition*, 651–660.
- Zhao, R.; Wang, V.; Kannala, J.; and Pajarinen, J. 2024. Grouped Discrete Representation Guides Object-Centric Learning. *arXiv preprint arXiv:2407.01726*.
- Zhao, R.; Wu, Z.; and Zhang, Q. 2021. Learnable Heterogeneous Convolution: Learning both Topology and Strength. *Neural Networks*, 141: 270–280.